ISSN 0016-7029, Geochemistry International, 2018, Vol. 56, No. 11, pp. 1051–1070. © Pleiades Publishing, Ltd., 2018.
Original Russian Text © N.M. Sushchevskaya, B.V. Belyatsky, D.A. Tkacheva, G.L. Leitchenkov, D.V. Kuzmin, A.V. Zhilkina, 2018, published in Geokhimiya, 2018, No. 11, pp. 1005–1025.

Early Cretaceous Alkaline Magmatism of East Antarctica: Peculiarities, Conditions of Formation, and Relationship with the Kerguelen Plume

N. M. Sushchevskaya[a], *, B. V. Belyatsky[b], **, D. A. Tkacheva[c], G. L. Leitchenkov[c, d], *, D. V. Kuzmin[e], ****, and A. V. Zhilkina[a]**

[a]*Vernadsky Institute of Geochemistry and Analytical Chemistry, Russian Academy of Sciences, Moscow, 119991 Russia*
[b]*Center for Isotopic Research, Karpinskii All-Russia Research Institute of Geology, St. Petersburg, Russia*
[c]*Gramberg All-Russia Research Institute of Geology and Mineral Resources of the World Ocean (VNIIOkeangeologiya), St. Petersburg, 190121 Russia*
[d]*St. Petersburg State University, St. Petersburg, 199034 Russia*
[e]*Sobolev Institute of Geology and Mineralogy, Siberian Branch, Russian Academy of Sciences, Novosibirsk, 630090 Russia*
**e-mail: nadyas@geokhi.ru,*
***e-mail: bbelyatsky@mail.ru,*
****e-mail: german_l@mail.ru,*
*****e-mail: kuzmin@igm.nsc.ru*

Received November 14, 2017; in final form, January 24, 2018

Abstract—Generalization of available literature and new original data showed that the Early Cretaceous high-Mg alkaline magmatism is confined to the ancient Lambert rift zone. Alkaline ultramafic rocks developed in the areas of this zone (Jetty Oasis, western flank of the Beaver and Radok lakes, Fisher and Meredith massifs) were derived through melting of metasomatized continental mantle at ~1270°C and at depths of 130–140 km. Variations of major and trace-element composition and the wide range in olivine composition (Fo_{91}–Fo_{80}) are consistent with its change through intrachamber crystallization. The average values of initial isotope composition of ultra-alkaline high-Mg basalts are as follows: $^{143}Nd/^{144}Nd$—0.512485, $^{87}Sr/^{86}Sr$—0.70637, $^{207}Pb/^{204}Pb$—15.671, $^{206}Pb/^{204}Pb$—18.391, $^{208}Pb/^{204}Pb$—38.409. They are close to the model *EMII* source and can be arbitrarily taken as the preliminary assessment of isotope composition of a source of Mesozoic melts. Based on lithophile element and isotope compositions, the alkaline high-Mg basaltic magmatism is thought to be related to the thermal impact of the Kerguelen plume on the lithospheric mantle of East Gondwana 120–110 Ma. Similar ancient deep-seated metasomatized eastern Gondwanan mantle, which contains carbonates and biotite and has an age of 2.4 Ga, was found in southern East Antarctica as well as in the north within eastern India.

Keywords: East Antarctica, Lambert Rift, Kerguelen plume, geochemistry of ultrabasic alkaline magmatism
DOI: 10.1134/S0016702918110071

INTRODUCTION

The passive continental margin of East Antarctica and adjacent oceans was formed through rifting and subsequent breakup of Gondwana (separation of Africa, India, and Australia from Antarctica). The evolution of this large region was mainly related to the activity of mantle plumes and hot jets, which are expressed in the morphostructures of ocean floor, potential fields, and geological (geochemical) specifics of oceanic lithosphere. The role of plumes in the present-day lithosphere evolution is obvious, whereas their influence on and interaction with continental crust at the rifting stage remains weakly studied and frequently ambiguous. The fundamental significance of this problem is determined by the possible cause-and-effect relationship between the mantle plume activity and the Gondwana break-up. The determination of style and volume of passive-margin magmatism makes it possible to estimate the influence of mantle plumes and hot spots on the crustal accretion and evolution, as well as to supplement and expand our knowledge of the general geodynamics of continental margins and oceans.

The Cretaceous ultrapotassic intrusions emplaced in the ancient sedimentary basins of Gondwana, in spite of the relatively well-studied mineralogy, are ascribed to the ambiguously classified rocks (Chalapathi Rao et al., 2014). They comprise such variously termed rocks as potassic biotite traps, biotite-bearing ultramafics, lamprophyre, glimmerite, lamproite,

Fig. 1. Rift grabens and Cretaceous magmatism of East Gondwana (reconstruction of continents at 115 Ma; Coffin et al., 2002; Veevers and Saeed, 2009, Leitchenkov et al., 2015, 2016). Continents are shown by dark gray color, continental margins, by light gray. Magmatic manifestations: (1) Bunbury, (2) Naturaliste Plateau, (3) Bruce Spur; (4) central part of the Prince Charles Mountains; (5) Rajmahal Province, (6) southern part of the Kerguelen Plateau. Dashed line shows the buried Cretaceous volcanic complexes of the Bengal Basin. Dotted line shows the inferred position of the Mahanadi and Lambert rifts. Circles outlines the region of lithosphere of East Gondwana of the inferred Kerguelen plume.

phlogopite and alkaline picrite, but represent a single group of deep-seated alkali-rich rocks formed in a continental setting. Cretaceous alkaline rocks developed within the Lambert Glacier in East Antarctica belong to the high-Mg alkali basalts (dolerites). They contain 29–36 wt % SiO_2, 12–20 wt % CaO, 3–6 wt % total alkalis, and are enriched in lithophile elements and volatiles (Andronikov and Foley, 2001; Sushchevskaya et al., 2016). These rocks will be further termed high-Mg alkaline basalts (ultramafic lamprophyres after (Andronikov and Foley, 2001), giving no sense in the use of accurate petrographic nomenclature for these rocks varieties.

Previous works on the Cretaceous alkaline rocks of Antarctica describe separate manifestations of this magmatism, without geochemical and petrological generalization of all available data. In addition, many analytical data on rock composition have not been published yet, being available only in the reports of Antarctic expeditions. Therefore, the main goal of this paper is to generalize characteristics of Cretaceous alkaline-ultrabasic magmatism on the basis of previous studies and new original data.

LAMBERT RIFT AND GELOGICAL COMPLEXES OF EAST GONDWANA

The Lambert rift, the East Antarctica's largest tectonic structure, is extended inland from the continental margin (Prydz Bay) for 700 km and traced by the valley of the Lambert outlet glacier within the Precambrian crystalline shield (Fig. 1, Leitchenkov et al., 2018). The Lambert Rift is the only geophysically and geologically proved riftogenic structure in East Antarctica (Kurinin and Grikurov, 1980). It is characterized by the well-expressed basement depression 50–80 km wide, thick (up to 10 km) sedimentary infill, and asymmetric flanks: the western flank is represented by the Prince Charles Mountains more than 2 km high, while the eastern flank is a gentle plain exposed at sea level (Kurinin and Aleshkova, 1983).

Geophysical data indicate the continuation of the Lambert Rift inland along the eastern foot of the Gamburtsev Mountains up to 85° S (Fig. 1, Leitchenkov et al., 2004; Ferraccioli et al., 2011; Leitchenkov et al., 2015). The northern continuation of this structure before the break-up of East Gondwana was the Mahanadi graben located in the northeastern part of the Hindustan Peninsula (Fig. 1, Veevers and Saeed, 2009). The Lambert Rift evolved for a long time from the end of Carboniferous to the middle Early Cretaceous and ceased its activity after opening of ocean between India and Antarctica about 120–130 Ma (Leitchenkov et al., 2018).

The rifting was accompanied by magmatic activity expressed in the emplacement of dikes and eruption of alkaline olivine—leucite basalts in the Late Carboniferous and Early Triassic (Hoffman, 1991; Mikhalsky and Sheraton, 1993; Leitchenkov et al., 2018). In the middle Early Cretaceous, alkaline ultramafic magmas formed an extended (40-km long) chain of stock-like and dike bodies in the Jetty Oasis, thus marking a submeridional zone of deep-seated faults bounding the eastern flank of the Beaver Lake graben (Laiba et al., 1987). Magmatism of similar composition and age was also described in the Mahanadi graben in India (Chalapathi Rao et al., 2014). Timing of the ultrabasic-alkaline magmatism (120–110 Ma) confined to the ancient Lambert rift structure corresponds to the active stage of the Kerguelen Plume within the eastern spreading part of the Indian Ocean. In previous works, this magmatism was related to the final stage of rift activity (Tingey, 1990; Mikhalsky and Sheraton, 1993), but later studies demonstrated that mantle melting and intrusive activity in this region were related to the Kerguelen mantle plume (Olierook et al., 2016; Sushchevskaya et al., 2011, 2017). Spatial alignment of magmatism with the rift structure in this case is determined by the elevated permeability of these structures for deep-seated magmas, which emphasizes the significance and role of upper lithosphere weakened zones in the distribution of plume magmas.

The first signs of mantle plume activity in East Gondwana began with the eruptions of Bunbury basalts (West Australia), about 136–130 Ma (Fig. 1), at the final stage of the formation of the rift zone between India and Australia. It is suggested that approximately at that time, volcanism occurred on the Naturaliste Plateau (southwestern Australian margin) and the conjugate Bruce Spur (East Antarctica margin). Maximum plume activity was expressed in the formation of the volcanic province in the southern Kerguelen Plateau between 120 and 110 Ma (Coffin et al., 2002). The geochemical similarity of ultra-alkaline magmatism of the Mahanadi graben and Jetty Oasis (Sushchevskaya et al., 2017) indicates that the manifestations of alkali basic magmatism along the periphery of the Kerguelen plume were generated through a single process.

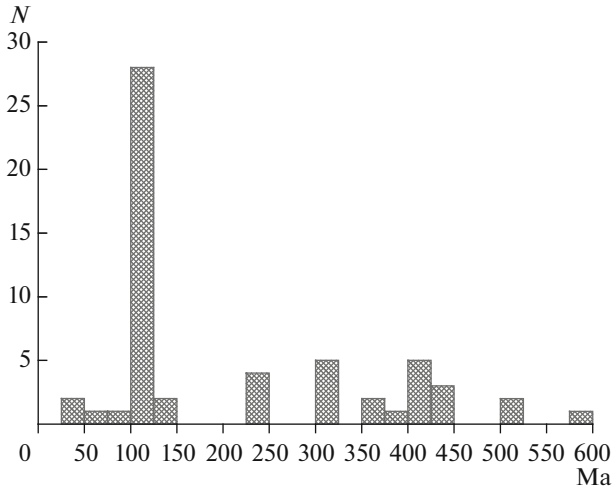

Fig. 2. Age frequency histogram for the magmatic rocks of the Lambert Rift. Constructed using data from (Hofmann et al., 1991; Mikhalsky and Sheraton .1993; Stephenson and Cook, 1992; Andronikov and Foley, 2001; Foley et al., 2002; Yaxley et al., 2013; Special Report no. 6202 by Krasnikov. Geological-geophysical works in the mountainous areas of Antarctica during 32 SAE, 1986–1987, vol. 2).

Presently available geochronological data on the magmatism of the Lambert rift zone are shown in Fig. 2 as the age frequency histograms compiled on the basis of available published data (over 60 individual datings on the alkali basalts, dolerites, and gabbros) and indicate a significant time range of magmatic activity within 50–500 Ma. Such a long-term magmatic activity can be related to the specifics of the evolution of rift zone (with elevated permeability and thinning of crust, increase of heat flux, and upper mantle upwelling), and with specifics of isotope systems used for dating. In particular, most of age determinations were obtained by K–Ar whole rock method for alkaline, subalkaline, and basite dikes, minor intrusions and sills, which makes allowance for the significant uncertainty associated with the obtained age values (Egorov et al., 1989; Andronikov et al., 1987; Hoffman et al., 1992) and requires further confirmation by independent isotope-geochronological methods. At the same time, we think this will be of great importance to demonstrate the entire spectrum of known dates to reveal the most reliable intervals of Mesozoic magmatism. The oldest ages were obtained for alkaline basites from the southern Prince Charles Mountains (three dates), Mount Bayliss (six datings), Taylor Platform (one dating), Jetty Oasis (four datings), and Kamenistaya Platform (two datings). However, most of the isotope dates on the magmatic rocks of the Jetty Oasis (and in general, of the rift zone of the Lambert Glacier) are within the time range of 120–110 Ma, thus reflecting the Early Cretaceous magmatic stage within East Antarctica.

METHODS

Olivines were analyzed by ion mass spectrometry on a CAMECA IMS-3f microprobe at the Max Planck Institute for Chemistry (Mainz, Germany) following technique (Migdisova et al., 2017) using accelerating voltage of the primary beam of negatively charged oxygen ions of 12.5 kV, accelerating voltage of the secondary ion beam of 4.5 kV, an offset 80 V, and a primary beam current of 300 nA. The energy slit at 25 V was centered. San Carlos olivine standard was used for calibration and accuracy assessment of measurements. All measurements of Si, Fe, Mn, Ni, Ca and Al were corrected for deviation of San Carlos standard from the reference values. For trace elements, the measurement conditions give detection limits of 6–15 ppm (3 sigma), and errors of 15–30 ppm for trace elements and 0.01 mol % for Fo content relative to olivine standard (Migdisova et al., 2017).

The contents of lithophile elements were determined at the Central Analytical Laboratory of GEOKHI RAS (Moscow) using developed original technique of open-system digestion of 100-mg samples. Brief description of the technique is given below. Weighed sample was placed into a 60-mL Teflon vial with a spherical bottom. The sample was mixed with a mixture of concentrated 4 mL HF and 1 mL HNO_3, and the vial was tightly closed by massive cap, and loaded in preliminarily heated (to a temperature of 50°C) volumetric heating block with a temperature controller and held for 72 hours. Samples of unknown composition were decomposed together with standard samples (BCR-2 and BHVO-2). To estimate the detection limits of elements, the procedure was carried out also for blank samples. After decomposition, the samples were evaporated at 140°C up to wet salts. Cooled samples were mixed with concentrated 2 mL HF and 0.5 mL $HClO_4$, then the vials were closed with caps having built up air refrigerator and were held for 12 hours at 140°C. When this procedure was finished, samples were evaporated up to wet salts. Then, they were mixed with a mixture of concentrated 1.5 mL HNO_3 and 1 mL HCl and heated to complete salt dissolution. Then, the solutions were evaporated to a volume of ~0.5 mL. Obtained solutions were placed in a plastic tube, and were added with 2% HNO_3 up to 25 mL. For ICP-MS, obtained solutions were additionally 20 times diluted by 2% HNO_3. Indium was added in solutions as internal standard to control drift of spectrometer sensitivity during the measurement. Concentration of the internal standard in samples was 10 μg/L.

The measurements were carried out on an XSeries II (Thermo Scientific) inductively coupled plasma quadrupole mass spectrometer at a plasma power of 1400 W, a plasma-forming argon (Ar) flow rate of 13 L/min, and auxiliary Ar flow rate of 0.95 L/min, Ar flow rate into a nebulizer of 0.87 L/min, and analyzed sample flow rate of 0.8 mL/min. Under such conditions, the level of oxide ions CeO+/Ce+ was no more than 2%, while the relative fraction of two-charged ions (Ba++/Ba+) is no more than 3%.

The measured spectra were processed using iPlasmaProQuad software (GEOKHI RAS), which provides import of all measured data into MS Access database and their processing by built-in facilities (including approximately 60 queries, with calculations). The processing includes plotting calibration curves, calculation of isotope concentrations, and introduction of corrections for the internal standard, control of measurement correctness, estimation of uncertainties (with allowance for error accumulation at different stages of analysis), consolidation of data, verifying for correction of analysis of standard samples and other functions. Data are given in Table 1.

The Sr, Nd, and Pb isotope compositions of rocks were determined at the Center for Isotopic Research of the Karpinsky All-Russian Research Geological Institute (Table 1). The elements were extracted using chromatographic and ion-exchange separation with previously described technique. The blanks during the measurements were no more than 0.01 and 0.1 ng for Rb and Sr, 0.02 ng for Sm and Nd, and 0.01 ng for Pb. The element contents were analyzed by isotope dilution with addition of calibrated isotope tracer. The isotope compositions of the elements were measured on a multicollector solid-state mass spectrometer TRITON TI (CIR VSEGEI) under a static regime. Normalizing values are $^{88}Sr/^{86}Sr = 8.375209$ and $^{146}Nd/^{144}Nd = 0.7219$. The isotope composition of standard JNdi-1 was as follow: $^{143}Nd/^{144}Nd = 0.512109 \pm 0.000006$; NIST-981: $^{206}Pb/^{204}Pb = 16.913 \pm 0.001$, $^{207}Pb/^{204}Pb = 15.451 \pm 0.001$, $^{208}Pb/^{204}Pb = 36.594 \pm 0.001$; NBS-987: $^{87}Sr/^{86}Sr = 0.710225 \pm 12$.

COMPOSITION OF ALKALI—ULTRABASIC ROCKS AND THEIR PETROGENESIS

Major-Element Composition of the Rocks

In the Jetty Oasis, the northern part of the Lambert Rift (Fig. 3), the stocks and dikes of alkaline-ultrabasic rocks cut cross the rocks of the Beaver Complex, Permian—Triassic terrigenous sediments of the Amery Complex, as well as Late Paleozoic weakly alkaline basic dikes (Mikhalsky and Laiba, 1990). Stocks of the alkaline-ultrabasic rocks in the Jetty Oasis at the modern erosion level are oval, more rarely equant in shape with size from 10 × 25 to 80 × 120 m, whereas the dike bodies reach 180 m long at thickness up to 2 m (Laiba et al., 1987; Andronikov, 1987). Detailed petrographic description of the rocks is given in (Grikurov et al., 1980; Egorov, 1994; Mikhalsky et al., 1998; 2007; Andronikov and Egorov, 1993; Kurinin et al., 1998).

Figure 4 shows the compositions of alkali rocks of the Lambert Glacier graben from data base, including analyses taken from published and closed-file reports of the Soviet and Russian Antarctic expeditions in the

Table 1. Contents of major element oxides (in wt %), trace lithophile elements (ppm) and isotope composition of alkaline-ultramafic basalts from the region of the Lambert Glacier

Element	Sample no.						
	P-3	C-3	AE 2/63	32 P-A51	32 YU-A44(1)	32 SV-A-41	32U-A5
	area/alkaline-ultramafic body						
	Ploskoe	Severnoe	Yuzhnoe	Lake Beaver	Yuzhnoe	Severnoe	Yuzhnoe
	rock						
	ol. melanephelinite	alk. picrite	Bi-Px picrite	lamprophyre	tuffobreccia	alk. picrite	alk. picrite
SiO_2	39.15	36.18	37.55	34.42	36.65	44.52	42.39
TiO_2	2.08	1.81	1.68	1.69	1.11	1.61	1.62
Al_2O_3	10.56	6.45	6.15	8.21	4.95	10.76	6.68
FeO	9.43	10.00	9.89	10.85	8.50	10.89	9.52
MnO	0.14	0.15	0.14	0.20	0.12	0.16	0.13
MgO	12.63	17.28	17.70	11.74	13.90	12.86	14.03
CaO	12.72	12.86	10.08	17.61	10.26	8.58	9.08
Na_2O	2.59	1.43	1.21	0.72	0.97	2.04	1.44
K_2O	1.87	1.62	2.06	2.96	1.69	2.10	1.89
P_2O_5	0.36	0.60	0.57	1.00	0.34	0.32	0.46
S	0.02	0.13	0.06	0.20	0.04	0.07	0.08
L.O.I.	7.77	11.26	13.14	9.04	22.43	4.61	12.55
Total	99.30	99.76	100.22	98.64	100.96	98.52	99.87
K_2O/Na_2O	0.79	1.28	1.96	4.55	2.26	1.09	1.51
CaO/Al_2O_3	1.20	1.99	1.64	2.15	2.07	0.80	1.36
Rb	67.8	59.3	86.2	144.1	106.5	8.3	100.2
Ba	1106.7	1301.9	1180	9974.7	155.7	97.3	217.0
Th	13.3	12.3	8.51	13.8	128.5	4.0	167.6
U	2.52	2.58	1.6	3.59	96.02	0.96	131.16
Nb	108.2	102.5	124	140.4	97.3	9.3	149.2
Ta	7.71	6.59	3.18	7.30	108.94	0.69	165.29
La	62.6	76.3	72.7	103.9	81.7	15.1	122.0
Ce	114.4	139.2	137	184.3	60.0	33.6	88.4
Pb	8.24	5.67	3.88	10.35	69.24	7.87	53.21
Nd	44.9	55.7	51.8	70.7	33.5	18.3	48.8
Sr	1046.5	929.2	738	3067.6	37.0	710.7	48.0
Sm	8.1	9.3	9.09	11.9	16.6	4.4	24.3
Zr	239.1	182.2	206	281.1	14.4	80.8	21.4
Hf	6.0	4.5	4.1	6.5	12.3	2.4	19.3
Eu	2.5	2.7	2.36	4.2	12.1	1.3	18.1
Gd	8.27	9.64	7	12.55	6.53	5.16	9.48
Y	20.0	19.3	18.3	32.8	3.3	26.6	4.6
Yb	1.62	1.44	1.30	2.46	2.49	2.88	3.50
Lu	0.23	0.20	0.16	0.36	2.34	0.43	3.18
Nb/Yb	66.62	71.25	95.38	57.01	39.08	3.22	42.62
Ce/Pb	13.88	24.55	35.31	17.80	0.87	4.28	1.66
Th/Yb	8.17	8.54	6.55	5.61	51.59	1.39	47.88
U/Pb	0.31	0.45	0.41	0.35	1.39	0.12	2.46
$^{87}Sr/^{86}Sr$	*0.70626*	0.70491	0.70621	*0.72921*	*0.70860*	*0.70732*	*0.71847*
$^{143}Nd/^{144}Nd$	*0.512644*	0.512683	0.512588	*0.512651*	*0.512530*	*0.512352*	*0.512577*
$^{206}Pb/^{204}Pb$	*18.719*	18.981	18.946	*18.622*	*18.7010*	*18.731*	*18.666*
$^{207}Pb/^{204}Pb$	*15.658*	15.654	15.681	*15.640*	*15.6796*	*15.792*	*15.662*
$^{208}Pb/^{204}Pb$	*39.180*	39.564	39.852	*38.981*	*39.0622*	*39.276*	*38.996*
$^{87}Sr/^{86}Sr$*	0.70578	0.70491	0.70621	0.72936	0.70860	0.70665	0.70605
$^{143}Nd/^{144}Nd$*	0.51255	0.51268	0.51251	0.51254	0.512426	0.51227	0.512474
$^{206}Pb/^{204}Pb$*	18.270	18.426	18.441	18.200	18.376	18.379	18.328
$^{207}Pb/^{204}Pb$*	15.603	15.627	15.656	15.619	15.664	15.766	15.663
$^{208}Pb/^{204}Pb$*	38.473	38.697	38.972	38.447	38.576	38.682	38.408

Average values from two measurements are shown in italics. * Data recalculated for an age of 117 Ma

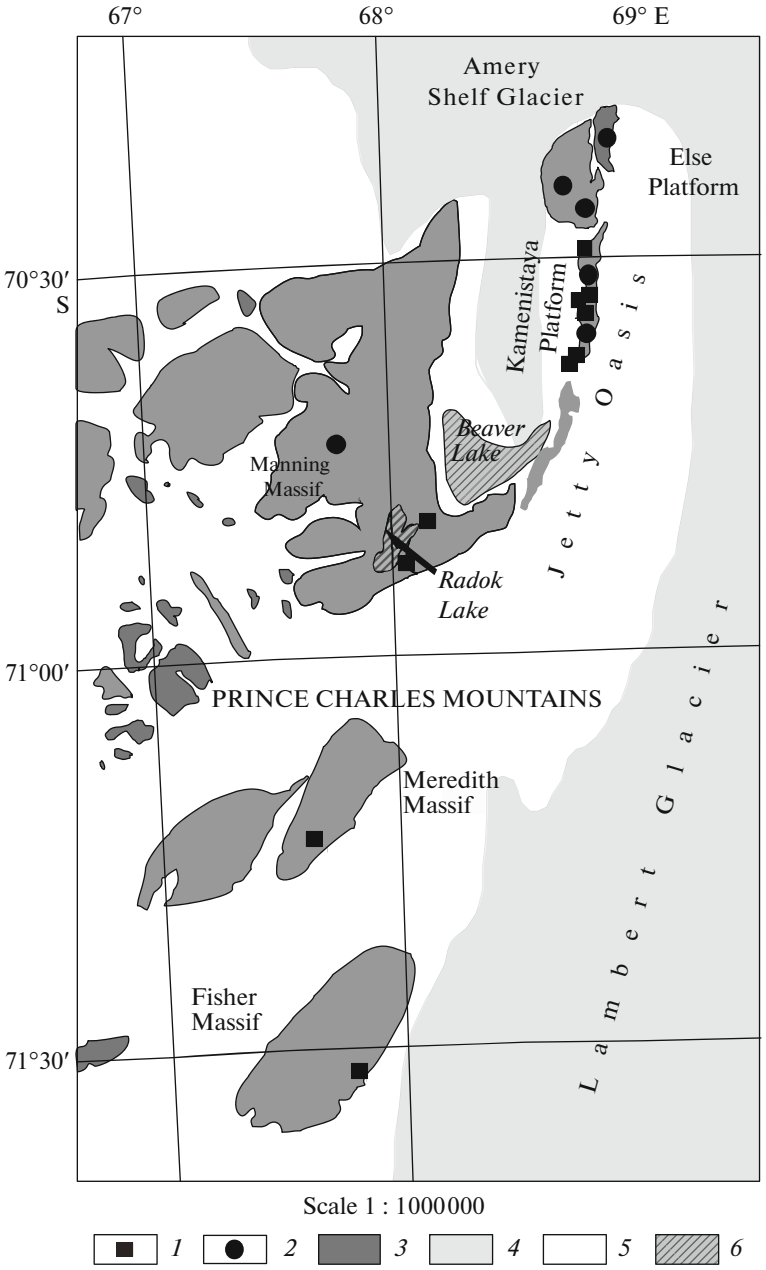

Fig. 3. Schematic map of the Lambert Glacier area with manifestation areas of Early Cretaceous magmatism: (*1*) Mesozoic (Cretaceous) magmatic bodies; (*2*) Pre-Cretaceous magmatic bodies; (*3*) exposures; (*4*) shelf and outlet glaciers; (*5*) continental glacial sheet; (*6*) lakes.

major component diagram. Starting data (about 300 analyses of Mesozoic rocks) were filtered by several parameters. For plotting, we used rock compositions with total over 90%, which then were recalculated to the water-free basis. Affiliation of rocks to the Mesozoic activity stage was sometimes determined from cross-cutting relations with host rocks, because geochronological determinations for these rocks are scarce. All samples (about 220 analyses) were conditionally subdivided into five groups according to their geographical position: (1) Jetty Oasis, eastern Beaver Lake, Kamenistaya Platform, south of the Else Platform; (2) Radok Lake, (3) Manning Massif; (4) western flank of Lake Beaver, and (5) Fisher and Meredith massifs (Fig. 3). The Manning Massif, whose leucite basalts have older ages (Leitchenkov et al., 2018), was also included in sampling for more complete comparison of peculiarities of alkali magmatism in this region.

Variation diagrams for major components (Fig. 4) indicate the presence of two rock groups: high-Mg group with MgO 10–27 wt % and low-Mg group with MgO from 9 to 2 wt %. The first group defines the

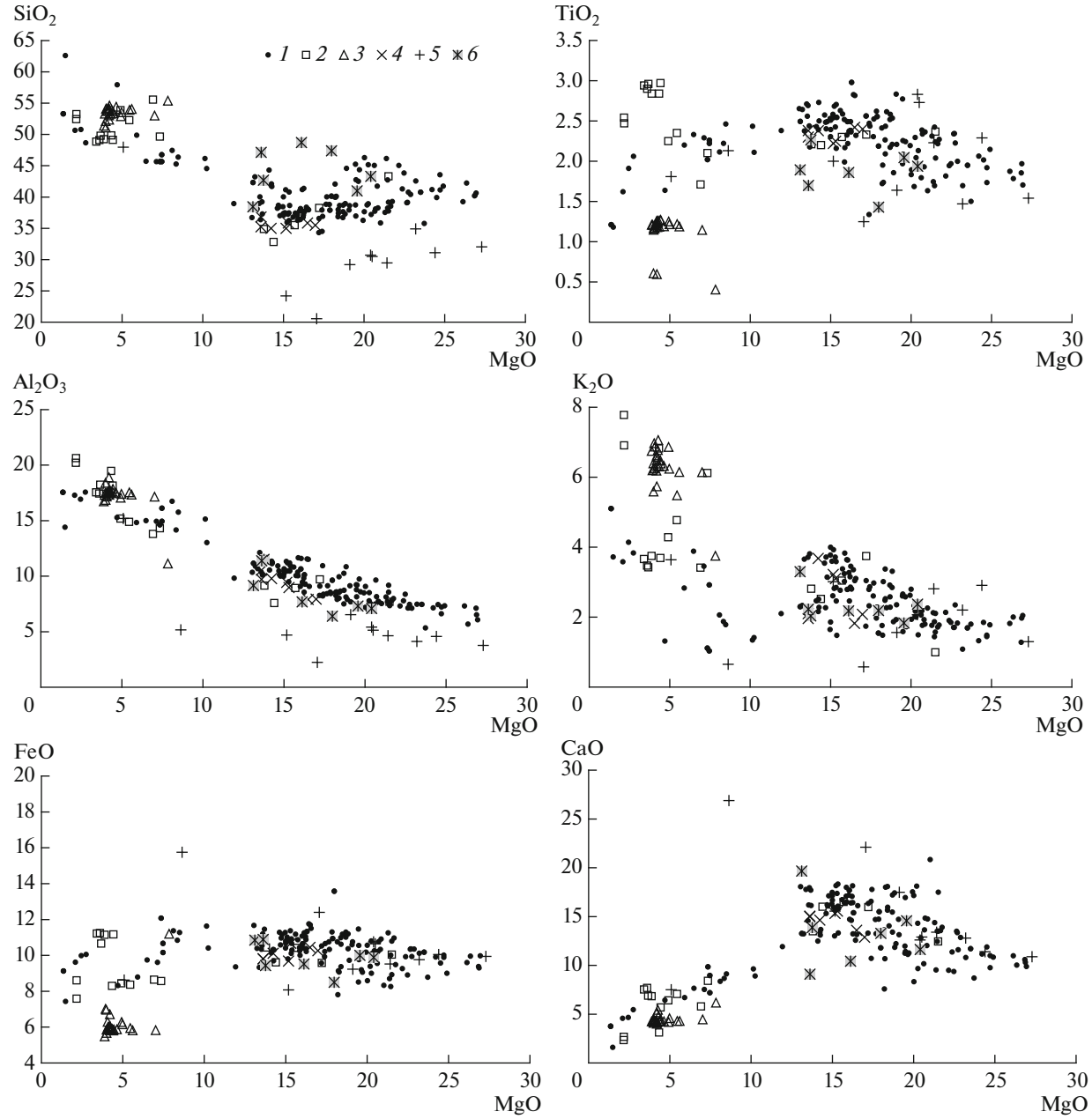

Fig. 4. Contents of major components in the alkaline rocks of the Lambert Glacier graben. Alkaline-ultrabasic basalts of the areas: (*1*) Jetty Oasis, eastern Beaver Lake, Kamenistaya Platform, and southern part of the Else Platform; (*2*) Lake Radok, (*3*) Manning Massif, (*4*) western flank of Lake Beaver, (*5*) Fisher and Meredith massifs, (*6*) new data presented in Table 1. Data were taken from (Andronikov, 1990; Mikhalsky et al., 1998; Alkaline—ultrabasic rocks of the Jetty Oasis and formation-geodynamic prerequisites for discovery of the kimberlite and carbonatite deposits on the Antarctic and other platforms: Report no. 99-110/Vniiokeanologiya, 1989; Kudryavtsev et al., 2006; Mikhalsky et al., 2001; Mikhalsky and Sheraton .1993; Stephenson and Cook, 1992; Andronikov and Foley, 2001; Foley et al., 2002; Yaxley et al., 2013)

clear trends of increase of Al_2O_3 (5–11 wt %), CaO (10–18 wt %), FeO (9–12 wt %), and TiO_2 (1.7–2.7 wt %) contents and less expressed trends of SiO_2 decrease (43–46% to 35 wt %). The total alkali increases from 2.7 to 6.7 wt %, while K_2O/Na_2O ratio varies from 0.4 to 2. There is a group with K_2O/Na_2O up to 4–5 and the lowered SiO_2 and Na_2O. This group is ascribed to the kimberlite rock association found in the Fisher and Meredith massifs (Laiba et al., 2007). The most representative group of high-Mg rocks is represented by the rocks of ultra-alkaline high-Mg association (ultramafic lamprophyres after (Foley et al., 2002), which is widespread in the Beaver and Radok lake areas. These rocks contain about 20–25% olivine, about 1–2% pyroxene, and about 5% titanomagnetite. The phlogopite content shows strong vari-

ations from sample to sample and may reach 10–15%, whereas the content of carbonate minerals (including secondary ones) reaches 10–20%, and over 30–40% in the most altered rocks. Accessory minerals are represented by apatite, ilmenite, monazite, pyrite, and other ore minerals (Andronikov, 1987). Revealed trends cannot be interpreted as the fractionation trends (for instance, with crystallization of magnesian olivine and pyroxenes), because the rocks are frequently cumulate in origin, which is reflected in the variations of mineral compositions within single sample, as well as in the presence of mantle xenoliths.

The second group of the rocks is less abundant and also shows an increase of Al_2O_3 (10–21 wt %) with decrease of CaO (from 10 to 1 wt %), FeO (from 12 to 5 wt %), TiO_2 (from 2.5 to 0.5 wt %), and increase of SiO_2 (from 45 to 60 wt %). The total alkalis also increase from 2.7 to 6.7 wt %, while the K_2O/Na_2O ratio varies from 0.4 to 2. Similar rocks were described in the Prince Charles Mountains, but as scarce finds were also observed in other regions. Similar rocks of alkaline andesite series were revealed in many regions of eastern Antarctica, where they are ascribed to ancient dikes (Sheraton, 1983; Sheraton et al., 1987; Tingey, 1991). They were also found in the Manning Massif area, where they were considered as the youngest magmatic rocks of the Lambert Glacier (40–50 Ma (Andronikov and Egorov, 1993; Andronikov et al., 1998)). However, recent U-Pb isotope dating showed that they are ascribed to the older magmatic rocks, at least to the Permian (Leitchenkov et al., 2018). It is possible that other dikes of similar composition are also older, but we cannot state this with confidence because they were described near and in the same areas where ultra-alkaline high-Mg magmas are developed.

Our study was focused on the high-Mg alkaline rocks, which gained the widest distribution and reflects an important stage of Mesozoic magmatism in Antarctica.

Variations in Olivine as Proxy to Source Composition

Olivines are the major liquidus phase of most mantle melts. Their major and trace-element composition depends on many reasons and can be used to establish the genesis and composition of parental melts (Foley et al., 2011, 2013; Sobolev et al., 2007). To determine the nature of liquidus olivines and their compositional variations during fractionation, we analyzed about 700 individual grains from five samples of alkaline high-Mg basalts and kimberlite from the Lambert Glacier graben. Figures 5–7 show variations of trace components for the studied olivine from separate samples and mantle inclusions in them. A wide range of Mg# (Fo_{91}–Fo_{80}, up to Fo_{74} in two cases) suggests that the olivine composition changed systematically during intrachamber crystallization (Fig. 5). The most magnesian olivines in alkali high-Mg basaltic melts are $Fo_{90–91}$. Figure 5 shows variations of NiO and Cr_2O_3 in olivine from separate samples of the studied lamprophyres, as well as in olivines from mantle inclusions. All the studied olivine fractions contain some amount of xenogenic olivine from disintegrated mantle xenoliths. Two samples of spinel lherzolites (mantle xenoliths in lamprophyres) have the lower Mg# ($Fo_{89–88}$) than would be expected for typical mantle olivines (Fig. 5, samples CH-A2, CH-H22). Such composition could result from either reaction processes, in which olivine significantly changed its initial composition, or analyzed olivine represents grains that were crystallized in thin metasomatized veinlets. Therefore, only studied olivine grains from spinel lherzolite 32U-A(1) from the "Yuzhnoe" stock-like body can be ascribed to typical mantle olivines. It is difficult to separate xenogenic olivines from liquidus ones, because they are similar in composition and contents of many components. In particular, the NiO and MnO contents in liquidus olivines (Fo_{91}) are about 0.4 and 0.12 wt %, respectively, which is close to mantle olivines (table with olivine compositions is given in Supplementary*). The Cr_2O_3 content in liquidus olivines increases up to 0.06–0.08% as compared to the typical mantle values of 0.025 (Figs. 5), as the CaO and TiO_2 contents. Cr behaves as Ni and reflects its decrease during fractionation. The absence of Cr_2O_3 correlation with olivine Mg# (sample 32U-A5) is likely related to the admixture of sulfides in magmas, which indirectly follows from the elevated Pb content (53 ppm). The CaO content in the liquidus olivines (0.10–0.12%) is typical of such magmas (Foley et al., 2013).

The MnO content during olivine crystallization systematically increases from 0.12 to 0.28–0.30 with Mg# variation within (Fo_{91-80}), while Al_2O_3, CaO, and Cr_2O_3 decrease from 0.6 to 0.01, from 0.12 to 0.04, and from 0.06 to 0.005, respectively. At the same time, olivine from sample U-22 shows two variation trends for Ni, Mn, and Al versus Mg#, which are likely related to a change of redox conditions of crystallization, which significantly affect the partition coefficients (Foley et al., 2011). The NiO content in the most magnesian olivines for all studied samples reaches 0.4 wt % and coincides with the NiO content in mantle olivines. It should be noted that the NiO content during fractionation increases by 10 times in the higher Fe varieties, reaching 0.04% in olivines Fo_{75}, which confirms a significant role of differentiation in olivine crystallization. Olivine partition coefficients for Ni strongly depend on the alkalinity and Mg # of melts and reach 30—40 for melts similar to the studied ones (at MgO content about 20%). With MgO decrease down to 9–10%, the coefficients could reach 50–60 (Foley et al., 2013).

Mantle olivines also differ in the low TiO_2 content (0.04%) as compared to magnesian liquidus olivines $Fo_{90–91}$, for which this value on average reaches 0.12%.

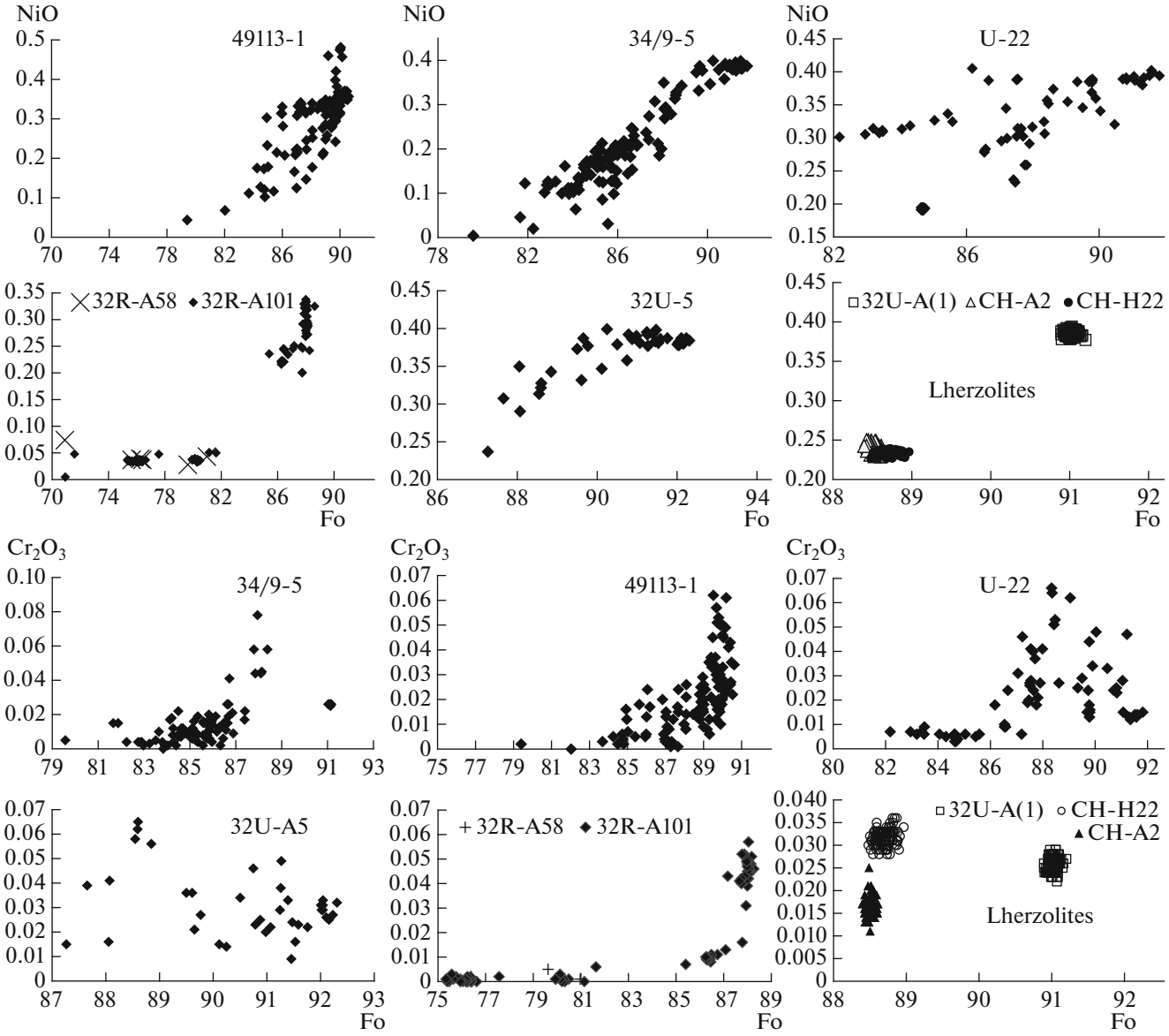

Fig. 5. Variations of NiO and Cr_2O_3 (wt %) in olivines from separate samples of alkaline ulramafic magmas of the Jetty Oasis and mantle xenoliths in them.

Figure 6 shows Ti–Ca variations in olivines from alkali ultrabasic rocks and mantle xenoliths in them. Separate samples show trends of increasing Ti and Ca contents during fractionation. Such trends are similar to the known dependences for olivines from continental alkali rocks and kimberlites (Foley et al., 2011). Olivines from mantle xenoliths define trends of increasing Ti–Ca, which are related to the metasomatic transformations, as well as an increase of Ti content against the background of insignificant growth of Ca. These trends were also described for olivines from hyperbasites in different geodynamic settings, including the Kaapvaal craton, mantle xenoliths in which also contain olivine with increasing Ti content (Foley et al., 2013).

As compared to the typical tholeiitic olivines of oceanic settings, the studied olivine (Sobolev et al., 2007) differs in the lower CaO and MnO, and higher NiO/CoO, on average 0.20, which is close to mantle values (Figs. 7a, 7b). In general, alkali ultrabasic magmas in terms of some parameters are close to mantle derivatives, but at the same time have own specifics, which reflect their more complex origin. In particular, the compositions of the studied olivines do not fall on the known mixing trend between pyroxenite and peridotite sources (Figs. 7c, 7d) (Sobolev et al., 2007), which likely indicates the presence of not only pyroxenite mantle, but also admixture of carbonates, phlogopite, and other fluid-bearing minerals in melt sources. Melting presumably occurred in the presence of carbonate minerals in residual peridotite, because Ca content in liquidus olivines is low (Fig. 7d), which reflects its low content in parental magmas.

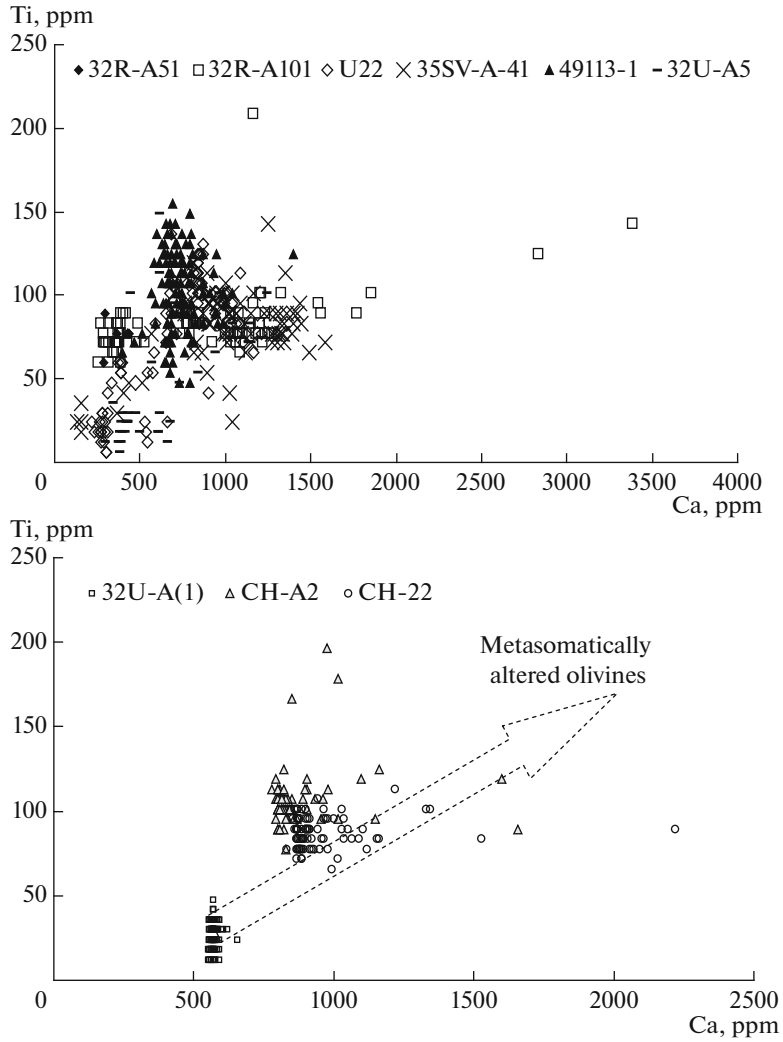

Fig. 6. Comparative characteristics of olivines from alkaline ultramafic rocks and mantle xenoliths in them (Ti and Ca contents). Arrow shows an increase of Ca content during metasomatic reworking of ultrabasite olivines after (Foley et al., 2013).

GEOCHEMISTRY OF ALKALINE ULTRABASIC ROCKS

Contents of Lithophile Elements in Magmas

Figure 8 shows the distribution of mantle-normalized lithophile elements for the studied samples of alkali high-Mg basalts from the Jetty Oasis. Most of the samples differ in the high degree of enrichment in the most incompatible elements as compared to more compatible elements. The elevated $(Gd/Yb)_N$ ratios within 2–8 indicate the possible presence of garnet in a protolith (Hofmann, 2003).

The characteristic negative Zr, Hf, and Nb anomalies could indicate the presence of rutile in the residual material. Practically all samples show variable negative U and Pb anomalies, which could be related to the removal of these elements with carbonate fluid. The lithophile element distribution in the kimberlite rocks is close to that of the studied samples of ultramafic lamprophyres (Fig. 8).

Observed high dispersion of lithophile elements for the alkali high-Mg basalts of the Lambert Rift reflects, first and foremost, the heterogeneous composition of a continental source and presumably variable but low melting degrees, as well as the influence of fluid regime, which could change during magma generation (Andronikov and Foley, 2001). Heterogeneity of samples with respect to the lithophile elements requires more comprehensive study. Due to the limited volume of taken samples, such study is presently impossible. Therefore, we only emphasize the main features of the trace element composition of the rocks. In particular, the characteristic Ce/Pb ratio for the significant part of samples is close to mantle value of about 20 ± 5 (Hofmann, 2003) (Fig. 9). Most samples show a trend of decreasing Ce/Pb ratio with increase of SiO_2, Pb, Yb, and other lithophile elements, which is related to

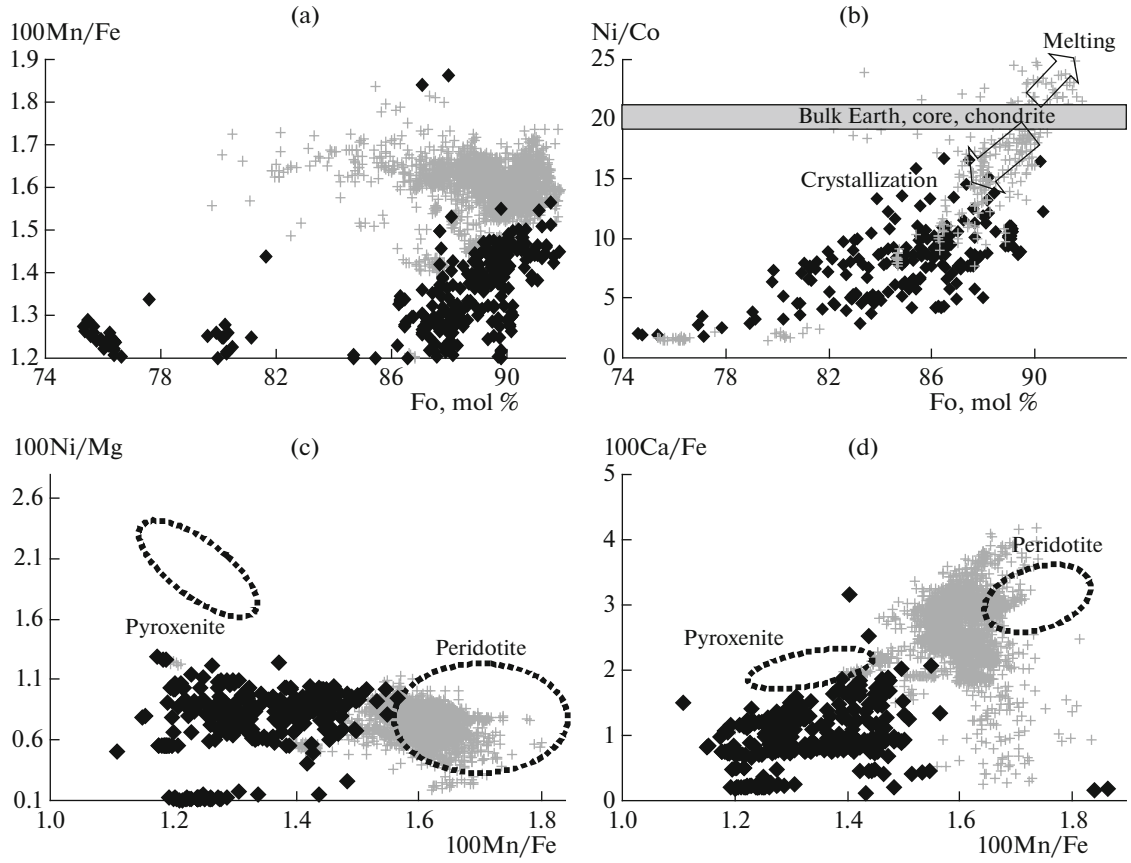

Fig. 7. Comparison of Ni, Co, and Mn contents in olivines from alkaline magmas of the Jetty Oasis and MOR tholeiites shown by gray crosses after (Sobolev et al., 2007). Fields show the composition variations of olivine in equilibrium with pyroxenites and peridotite sources after (Sobolev et al., 2007).

the fractionation accompanied by the increase of more compatible elements and decrease of incompatible elements, for instance, Ce and Ba (Figs. 9c, 9d). The fractionation is likely assisted by fluid, which could remove these elements. The fractionation and accumulation of the more compatible elements are reflected in the increase of characteristic ratios of more compatible to less compatible elements (e.g., Th/U ratio, Fig. 9a). The absence of significant correlation between Ce/Pb ratio and Pb isotope composition indicates the isotopically homogenous composition of magma source. The low Ce/Pb ratios are typical of magmas with elevated SiO_2 contents (Fig. 9b). These are samples from the "Yuzhnoe" stock-like body (32U-A5 and 32YU-A44(1)), which have the highest $^{207}Pb/^{204}Pb$ (Fig. 9f, outlined rhombs). The lithophile element distribution pattern in the latter sample strongly differs in the positive Th, U, Yb, and Y anomalies and the lowered contents of the least incompatible elements (Fig. 8).

Pb–Sr–Nd ISOTOPE CHARACTERISTICS OF MAGMATISM

The isotope characteristics of basites are of great importance for understanding the genesis of Cretaceous magmatism in the Lambert Glacier area. Diagrams in Fig. 10 show the isotope compositions of bulk samples recalculated for their age, as well as the initial isotope characteristics of kimberlite rocks of the Fisher massif located 140 km south of the Jetty Oasis (Yaxley et al., 2013). For comparison, we showed the initial isotope compositions of the ultra-alkaline basic trachyandesites of the Triassic Manning Massif (Leitchenkov et al., 2017) and Jurassic lamproites of the Ferrar Province (West Antarctica, Elliot et al., 1999), which are related to the magmatism of the Karoo–Maud plume (183 Ma), and Cenozoic lamproitic lavas of the Gaussberg Volcano (Wilhelm II Land). In all presented diagrams, the isotope compositions of Cretaceous basites define a compact field, which is separated both from the composition of older alkaline rocks, including Triassic volcanic rocks of the Manning Massif and Jurassic lamproites of the Ferrar Province (Elliot et al., 1999), and from the younger lamproites of Australia (20 Ma, Mirnejad and Bell, 2006) and volcanic rocks of Gaussberg Volcano (Sushchevskaya et al., 2014). Moreover, we may conditionally recognize the variation trends, the depleted end-member of which with moderately radiogenic Nd, Sr, and Pb composition is similar in composition

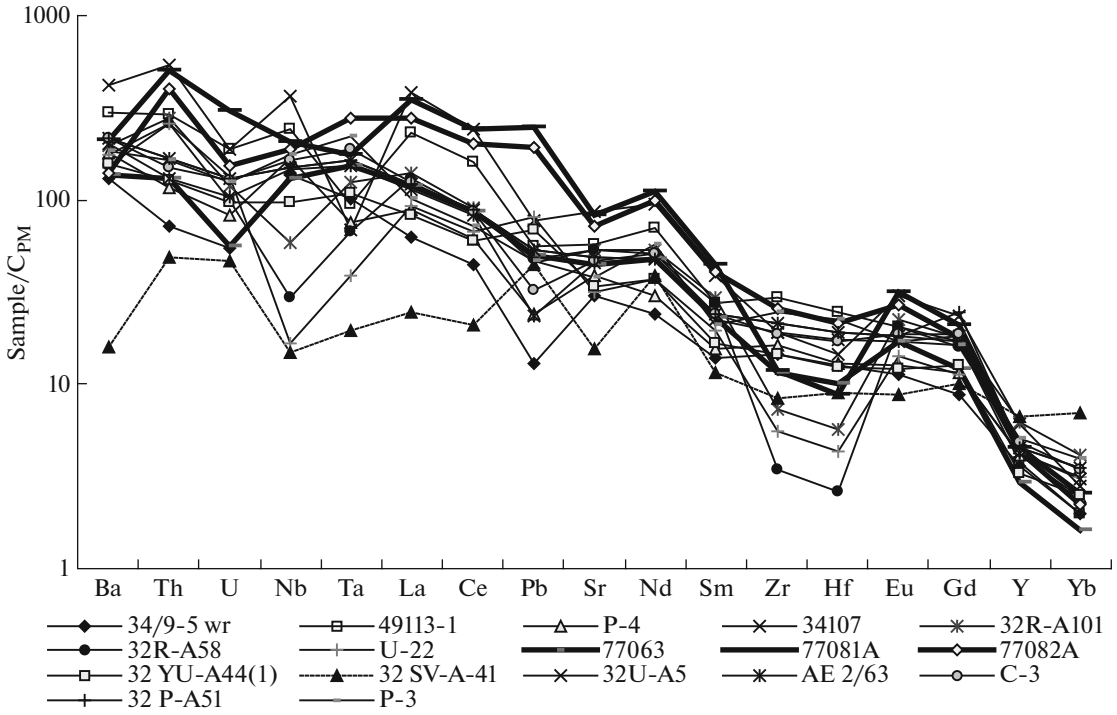

Fig. 8. Distribution of lithophile elements in the alkaline ultramafic rocks of the Jetty Oasis. Analysis data are shown in (Sushchevskaya et al., 2017) and Table 1, normalized to primitive mantle after (Sun and McDonough, 1989). Bold lines show variations of lithophile elements in kimberlites of the Meredith massif (Yaxley et al., 2013).

to kimberlites of the Fisher Massif or Jurassic lamproites of the Ferrar Province (kimberlite source KS in Fig. 11), while enriched end-member source with non-radiogenic Nd isotope composition and radiogenic Sr and Pb is similar to the most radiogenic varieties of leucite basalts of the Gaussberg Volcano or lamproites of Australia (sources II and III in Fig. 11). It should be noted that the studied ultra-alkaline magnesian basalts are isotopically most close to the kimberlite rocks of the Fisher Massif with the average isotope compositions of $^{143}Nd/^{144}Nd$—0.512523, $^{87}Sr/^{86}Sr$—0.70487, $^{206}Pb/^{204}Pb$—18.612, $^{207}Pb/^{204}Pb$—15.624, $^{208}Pb/^{204}Pb$—39.647 (KS in Fig. 11). The average values of the initial isotope composition of ultra-alkaline magnesian basalts are as follows: $^{143}Nd/^{144}Nd$—0.512485, $^{87}Sr/^{86}Sr$—0.70637, $^{207}Pb/^{204}Pb$—15.671, $^{206}Pb/^{204}Pb$—18.391, and $^{208}Pb/^{204}Pb$—38.409, and can be arbitrarily taken as the preliminary assessment of isotope composition of sources of Mesozoic melts (lamprophyric source, LS, in Fig. 11). The studied sampling is obviously characterized by a wide scatter of compositions, which may indicate mixing of different isotope components in a melt source (ancient lithospheric mantle, the plume component with high $^{238}U/^{204}Pb$), as well as significant influence of postcrystallization or intrachamber transformations owing to the high partial fluid pressure (presence of sulfides, and carbonates, late secondary alterations of rocks with input of nonradiogenic lead or excess uranium). In terms of all isotope characteristics, the ultra-alkaline magnesian basalts and kimberlites are close to a model *EMII*-type mantle source. At the same time, more accurate identification of source of enriched magmas is sufficiently difficult, because genetically diverse melts from different depths (kimberlites and lamproites) have similar isotope and trace element composition.

DISCUSSION AND GEODYNAMIC INTERPRETATION

The studied compositions of liquidus olivines are close to those of mantle xenoliths transported by magnesian ultra-K magmas. Similar isotope characteristics of ultrabasite xenoliths from lavas and proper basalts (Sushchevskaya et al., 2017) in the first approximation may indicate that lava source was mantle compositionally similar to mantle xenoliths brought by generating magmas. This is the case if such mantle is developed to a depth of 130–140 km, where melts were generated according to Foley et al. (2002). Based on alumina content in liquidus olivines and coexisting spinels (Coogan et al., 2014), the generation temperature of the Antractic lamproite magmas related to the Kerguelen plume reach 1270°C (Migdisova et al., 2018).

Obtained results indicate that the alkaline high-Mg basalts were derived through deep-seated melting of metamorphosed ultrabasic mantle. Enrichment of

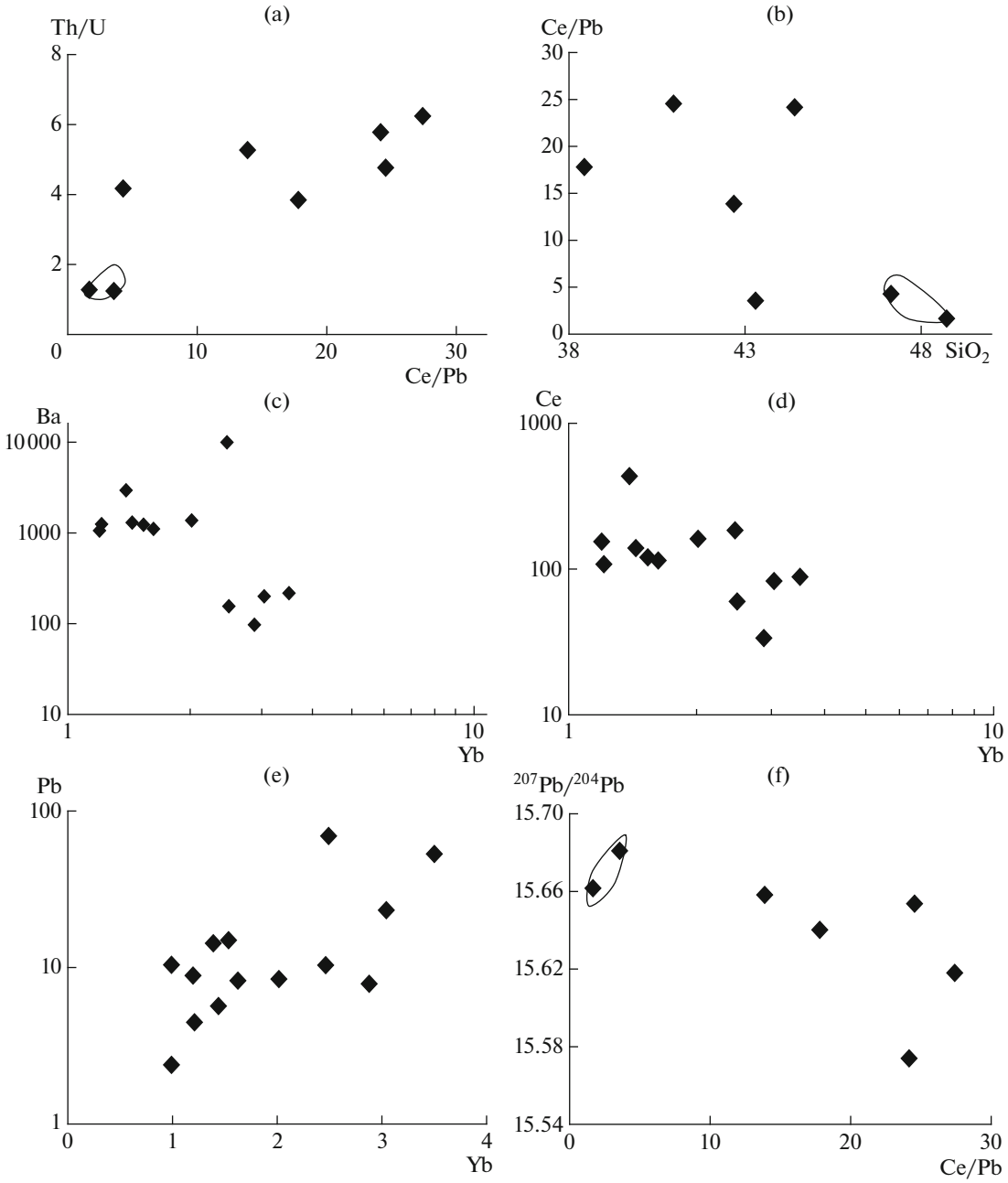

Fig. 9. Variations of Ba, Ce, Pb, Yb, Th/U, Ce/Yb, SiO_2 and $^{207}Pb/^{204}Pb$ in the alkaline ultramafic rocks of the Jetty Oasis.

melts in volatiles (Sushchevskaya et al., 2017) can be determined from the relative enrichment of mantle source in volatiles. The study of mantle xenoliths from the Jetty Oasis revealed that they contain CO_2 dominated fluid of complex composition. It was assumed that the fluids were formed in several stages, while an increase of H_2O in late fluid and argon isotope composition ($^{40}Ar/^{36}Ar$) indicate its subduction nature (Buikin et al., 2014).

The multiple interaction of mantle with fluid-saturated penetrating melts resulted in the formation of amphibole—phlogopite—apatite veinlets, i.e., minerals containing volatiles and lithophile elements (Ionov et al., 1997). Figure 12 shows covariations of Rb/Sr, Ce/Nb, Ba/Ce, and Nb/Th ratios, which depend on the admixture of phlogopite (high Rb/Sr), apatite (high Ce/Nb), or amphibole (high Nb/Th) in a source (according to (Ionov et al., 1997). Based on some parameters (Ce/Nb, Ba/Ce, Nb/Th), the alkaline magmas of the Lambert Rift are close to primitive mantle (Sun and McDonough 1989), but differ in the elevated Rb content and high Rb/Sr ratio (Fig. 9c). It is hardly possible to determine the proportions of min-

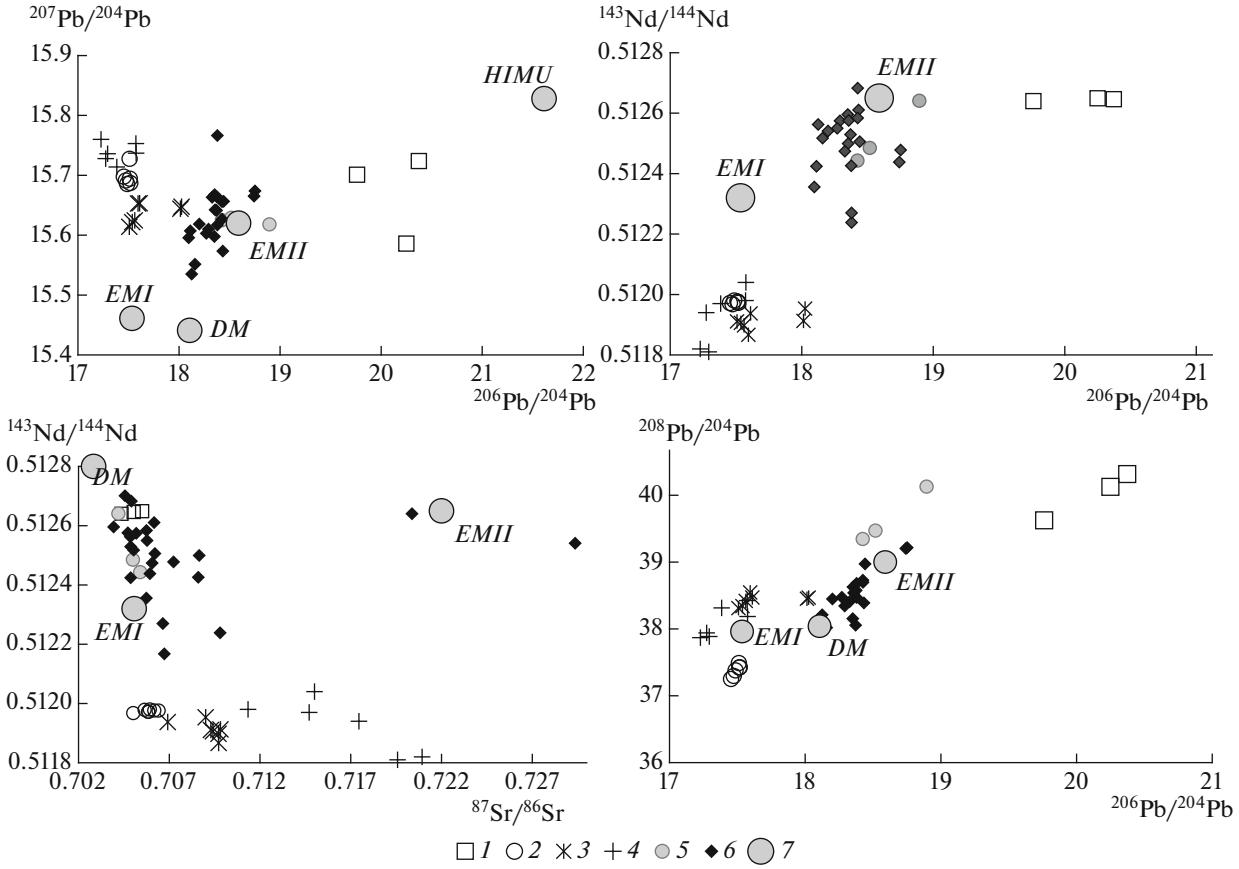

Fig. 10. Pb–Sr–Nd isotope characteristics of Mesozoic magmatism of the Lambert Rift. Alkaline ultramafic rocks of the areas: (*1*) lamproites of the Ferrar Province (Transantarctic Mountains, Antarctica); (*2*) olivine leucitites of the Manning Massif; (*3*) lamproitic rocks of Mt. Gaussberg; (*4*) Lamproites of Australia; (*5*) alkaline ultramafic rocks of the Lambert Rift; (*6*) kimberlites; (*7*) model enriched components after (Armienti and Longo, 2011). Data were taken from Table 1 and Elliot et al., 1999; Sushchevskaya et al., 2014, 2017; Yaxley et al., 2013; Mirnejad and Bell, 2006**;** Leitchenkov et al., 2017**.**

erals involved in melting due to their extremely uneven distribution in a space. In addition, while percolating through mantle matrix, fluid-rich melts cause significant mantle heterogeneity owing to so-called chromatographic effect (Ionov et al., 1997).

The fact that the kimberlite rock associations were found in the area of the Meredith Massif located south of the Beaver and Radok lakes may serve as an indirect evidence for the southward propagation of the Kerguelen Plume in East Antarctica, because kimberlites usually mark the plume periphery (Comin-Chiaramonti et al., 1997). A similarity of kimberlites to the alkali ultramafic rocks in terms of isotopic and rare-metal characteristics indicates that the deep-seated mantle of similar composition is extended up to this region.

The comparison of presented isotope variations of the studied magmas of the Lambert Rift and mantle xenoliths brought by alkali magmas of the Kerguelen plateau and Jetty Oasis, as well as variations in magmas related to the Kerguelen plateau (Sushchevskaya et al., 2017) showed that the mantle xenoliths and magmas are isotopically identical (Fig. 13). These isotope characteristics correspond to the ancient volatile-rich mantle source. The study of the Os isotope composition of mantle xenoliths from the Lambert alkaline ultrabasic rocks showed that the mantle in the East Antarctic region was formed no later than 2.5–2.4 Ga (Krymsky et al., 2011), whereas Sm–Nd isotope systematic of xenoliths suggests initial similarity of mantle composition with model chondrite uniform reservoir formed about 4.2 Ga. The later generation of silicate melts led to the formation of LILE-depleted lithospheric mantle existing without significant changes up to 2.5–2.4 Ga, when its thermal erosion and partial melting caused a change of Sm/Nd ratio in separate mantle domains (Belyatsky and Andronikov, 2009). The boundary of 2500–2400 Ma was marked by the emplacement of granite intrusions in the Enderby Land and the Prince Charles Mountains, deformations, re-equilibration of isotope systems, and low-grade granulite metamorphism, at high content of water, carbon dioxide, and other volatiles. This event was completed by the intrusion of tholeiitic dikes in

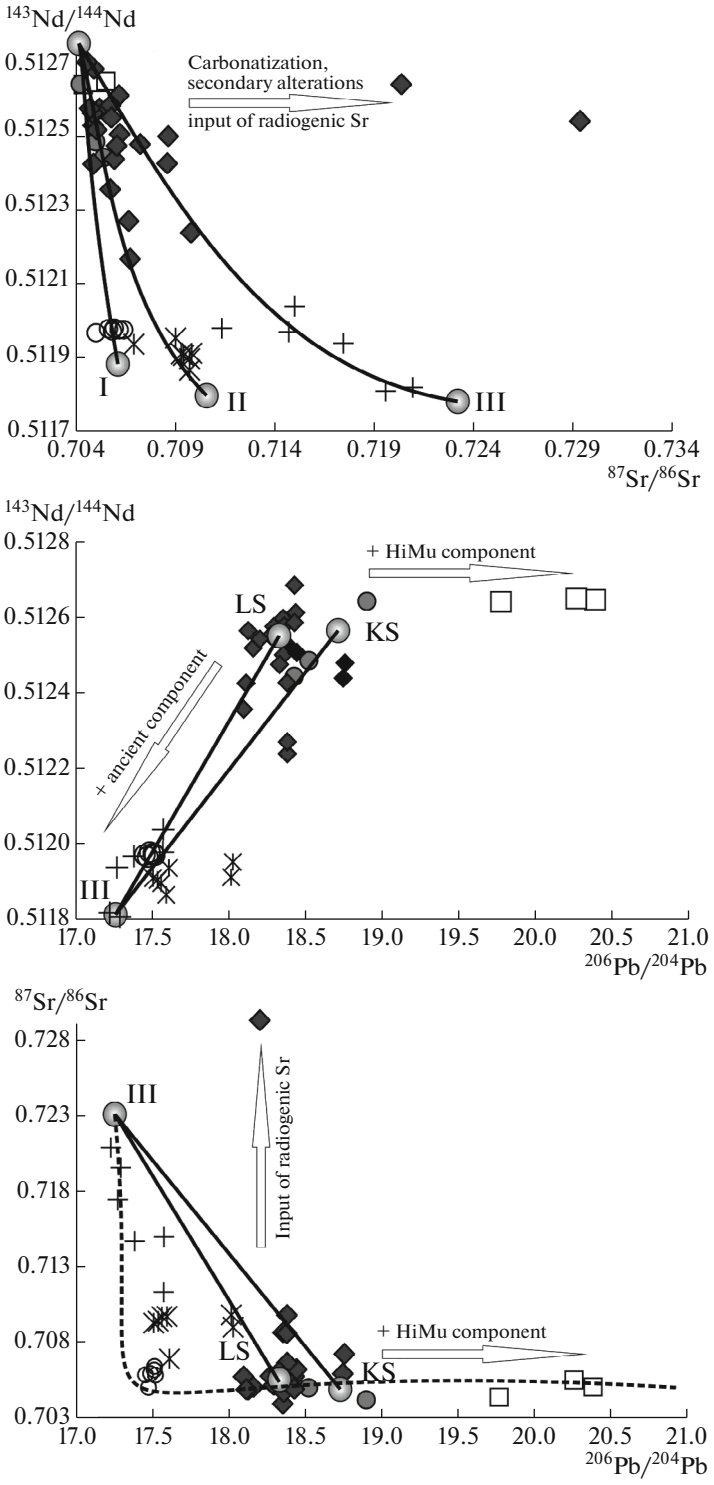

Fig. 11. Isotope characteristics of possible sources of Mesozoic alkaline-ultrabasic magmatism of the Lambert Rift. Lines in the figure show the possible mixing trends of mantle sources during formation of isotope composition of alkaline-ultrabasic magmas. Curves in the lower diagram correspond to mixing between mantle sources of Australian lamproites (III) and plume source (HIMU) at Sr/Pb ratio in a mixed source of III/HIMU about 100/1. I, II, III, KS, LS are inferred enriched mantle sources for leucite basalts of the Manning Massif, lamproite lavas of Gaussberg Volcano, Australian lamproites, as well as kimberlite and lamproite sources of Mesozoic magmas of the Lambert Rift, respectively. Arrows show an increase of influence of definite component/process during formation of isotope characteristics of the studied basites. Other symbols are shown in Fig. 10.

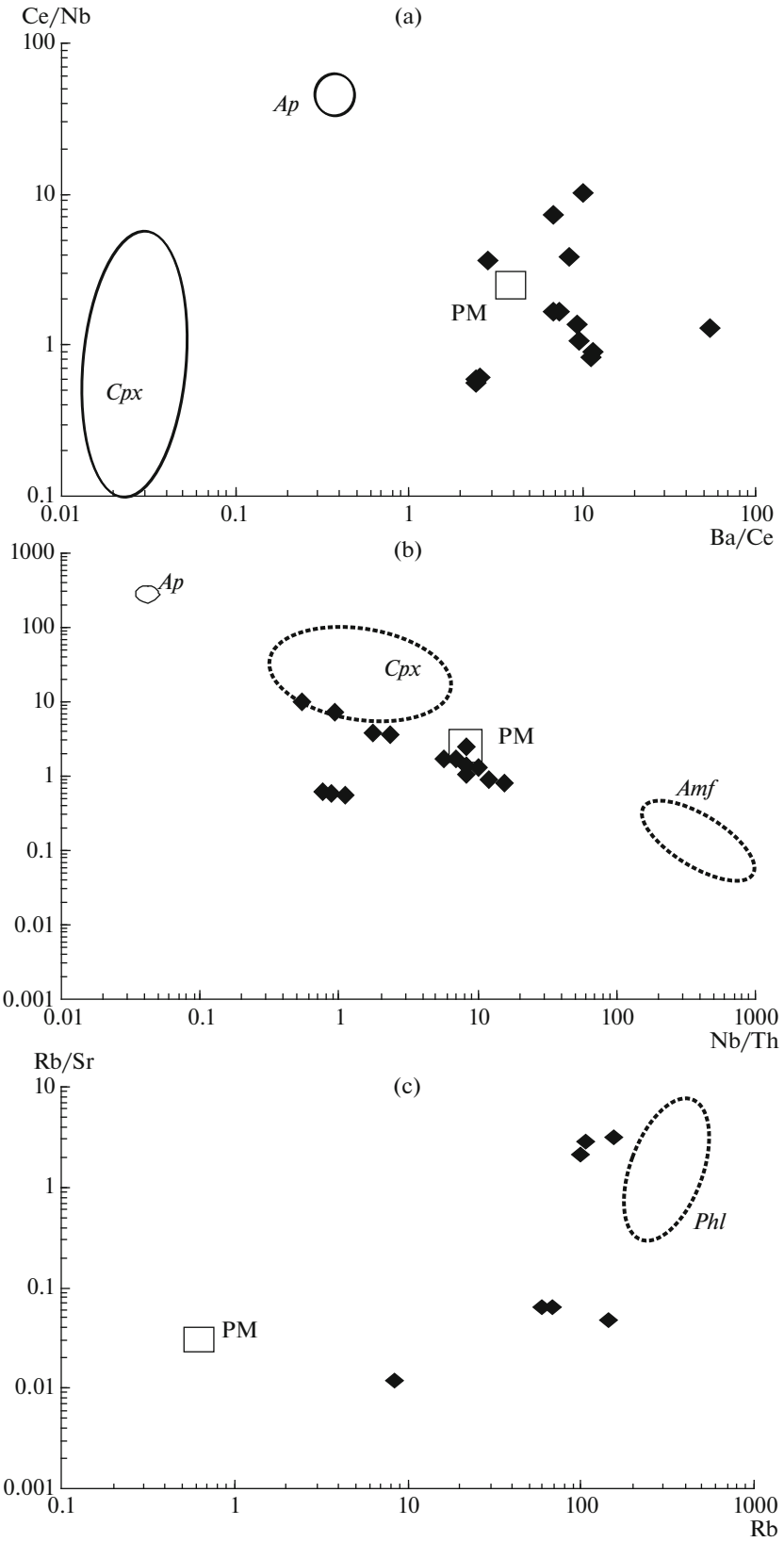

Fig. 12. Covariations of Rb/Sr, Ce/Nb, Ba/Ce, and Nb/Th in the alkaline basalts of the Jetty Oasis. Fields show variations of mantle components: clinopyroxene (*Cpx*), phlogopite (*Phl*), apatite (*Ap*), after (Ionov et al., 1997), and primitive mantle—PM (Sun and McDonough 1989).

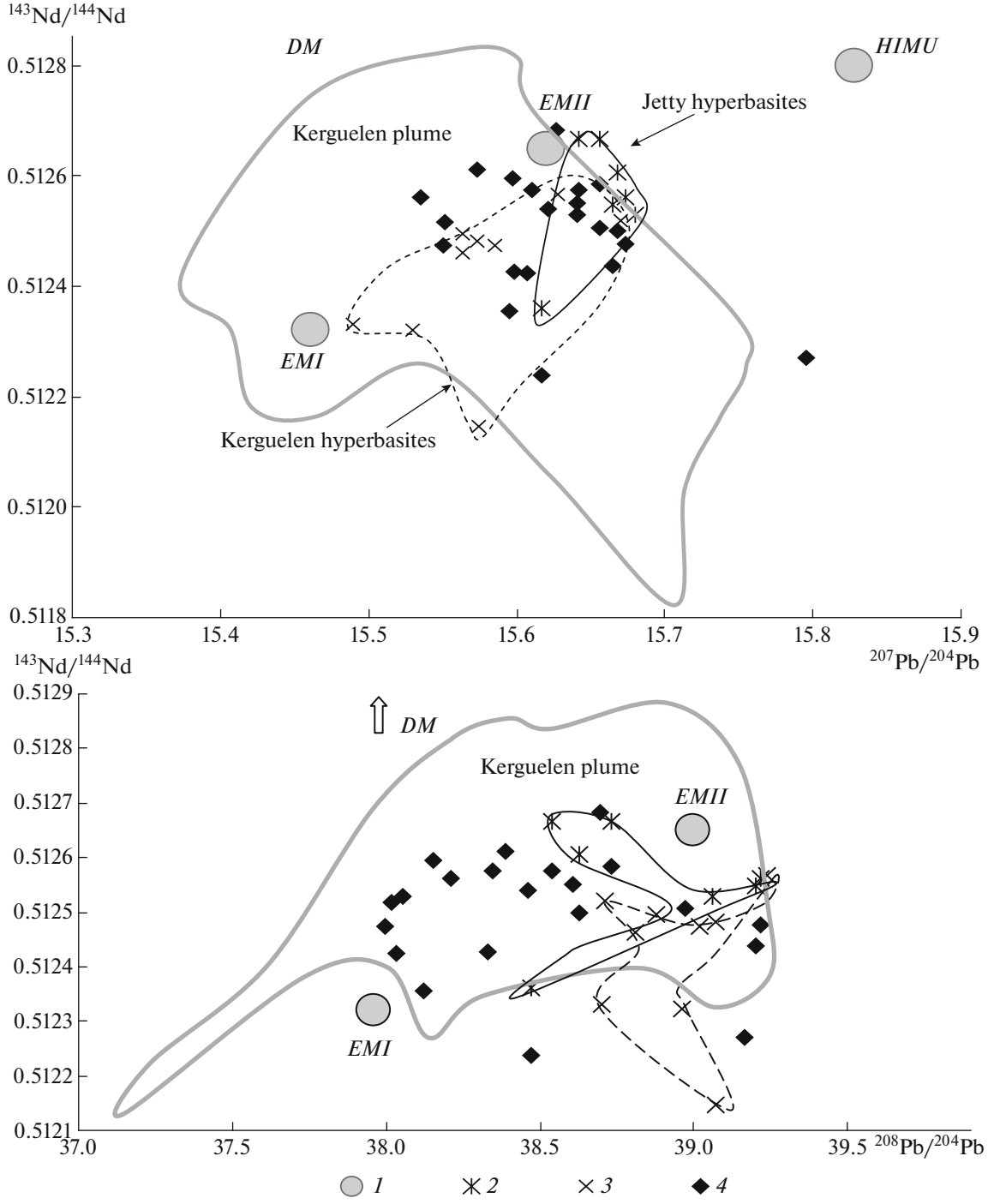

Fig. 13. Variations of isotope ratios in magmas of the Lambert Rift as compared to those of mantle xenoliths brought by the alkaline magmas of the Kerguelen Plateau to the surface (Sushchevskaya et al., 2017). Model enriched components after (Armienti and Longo, 2011) (*1*); isotope ratios in hyperbasite xenoliths from alkaline ulramafic rocks of the Jetty Oasis (*2*), and basalts of the Kerguelen plateau (*3*), isotope composition of alkaline ultramafic melts of the Jetty Oasis (*4*). According to data from Table 1 and from (Sushchevskaya et al., 2017).

the southern Prince Charles Mountains and Vestfold Oasis at 2350 Ma (Belyatsky and Andronikov, 2009; Veevers, 2012). It is pertinent to mention that a subcratonic mantle of similar age was also established beneath eastern India, for instance, in the northern Madurai Block (Plavsa et al., 2012), which according to Gondwana reconstructions, adjoined to East Antarctica (Harrowfield et al., 2005).

From 2.4 to 1.1 Ga, the lithospheric mantle of the region did not experience significant changes, which

indicates the greater resistance of the upper mantle and stability of conditions existing up to the continent–continent collision (between India and East Antarctica), and formation of Proterozoic mobile belts at 1.1 Ga. The last event is recorded in the isotope systematics of practically all studied xenoliths and reflects the total enrichment of the upper mantle horizons (likely, through subduction of oceanic lithosphere) and separation of xenolith source from a depleted mantle reservoir with formation of veined mantle.

Thus, the alkali high-Mg magmatism of the paleorift zone of the Lambert Glacier is related to melting of ancient metamorphosed mantle that is similar to the Kerguelen Plateau mantle, which was characterized on the basis of study of mantle xenoliths, or to the subcratonic mantle of eastern India. This emphasizes the relationship of enriched characteristics of alkaline and tholeiitic magmas with the Kerguelen plume, the thermal impact of which on the margins of spreading continental blocks of India and East Antarctica at 120–110 Ma led to the melting of deep-seated portions of volatile-rich mantle formed at the early stages of the formation of Gondwana paleocontinent.

CONCLUSIONS

Generalization of available published and new original data showed that the Cretaceous magmatism (120–110 Ma) is confined to the northern termination of the Lambert Glacier representing the ancient rift zone. This zone includes the Jetty Oasis, the western flank of Beaver Lake, Radok Lake, and Fisher and Meredith massifs. This zone contains mainly ultra-alkaline high-Mg associations formed through melting of metasomatized continental mantle at 1270°C and at depths of 130–140 km. Kimberlite rock associations found in the Meridith Massif area are close to the alkaline high-Mg magmas in terms of isotope and trace-element characteristics, which indicates that the deep-seated mantle of similar composition characterizing of the eastern Gondwanan mantle is extended southward of East Antarctica, as well as northward, in the East India.

The study of olivines from alkaline ultramafic rocks and mantle xenoliths in them showed that the liquidus high-Mg olivines ($Fo_{90–91}$) are close to olivines from xenoliths in terms of many trace components. The high Ni/Co ratios in them are close to mantle values, which points to a mantle origin of their magma source. At the same time, this source contained carbonate, biotite, and volatiles, while enriched ultra-alkaline high-Mg magmas and kimberlites from this source are similar in LILE distribution and Nd–Pb isotope characteristics.

Melting of such metasomatized mantle formed beneath the northern part of the Lambert Glacier about 2.4 Ga (Belyatsky and Andronikov, 2009) owing to the thermal impact of the Kerguelen plume about 120–110 Ma was responsible for the initiation of alkaline high-Mg magmatism within the ancient rift zones in East Antarctica and India.

ACKNOWLEDGMENTS

This work was supported by the Russian Science Foundation (project no.16-17-10139). The development of analytical techniques and softwares for processing of mass-spectrometric data was supported by the Russian Foundation for Basic Research (project no. 16-03-01079).

REFERENCES

Alkaline-Ultrabasic Rocks of the Jetty Oasis and Formation-Geodynamic Prerequisites in Revealing Kimberlite and Carbonatite Deposits at the Antarctic and other Platforms: Report of NIR (VNIIOkeanologiya, Leningrad, 1989) [in Russian].

A. V. Andronikov, "Mantle minerals from alkaline–ultrabasic rocks, East Antarctica," *Geological–Geophysical Studies in Antarctica* (PGO Sevmorgeologiya, Leningrad, 1987), pp. 48–53 [in Russian].

A. V. Andronikov, Extended Abstract of Candidate's Dissertation in Geology and Mineralogy (LGU, Leningrad, 1990) [in Russian].

A. V. Andronikov and L. S. Egorov, "Mesozoic alkaline-ultrabasic magmatism of Jetty Peninsula," *Gondwana Eight: Assembly, Evolution, and Dispersal*, Ed. by R. H. Findley, R. Unrug, M. R. Banks, and J. J.Veevers (Rotterdam, Balkema, 1993), pp. 547–558.

A. V. Andronikov and S. F. Foley, "Trace element and Nd-Sr isotopic composition of ultramafic lamprophyres from the East Antarctic Beaver Lake area," Chem. Geol. **175**, 291–305 (2001).

P. Armienti and P. Longo, "Three-dimensional representation of geochemical data from a multidimensional compositional space," Int. J. Geosci. **2**, 231–239 (2011).

B. V. Belyatsky, and A. V. Andronikov, Deep-seated inclusions of lherzolites from alkaline-ultrabasic rocks in the Jetty Oasis (East Antarctica): mineralogical-geochemical composition, P–T conditions, and Sr–Nd isotope characteristics," *Scientific Results of the Russian Geological–Geophysical Studies in Antarctica,* Ed. by E. V. Mikhalsky and A. A. Laiba (VNIIOkeanologiya, St. Petersburg, 2008), vol. 2, pp. 89–109.

B. V. Belyatsky, and A. V. Andronikov, "Age of upper mantle of the Beaver Lake area (East Antarctica): Sm-Nd isotope systematic of mantle xenoliths," *Problems of Arctic and Antarctica* **78** (4), 146–169 (2009).

A. I. Buikin, L. N. Kogarko I. P. Solovova, A. B. Verchovsky, and A. A. Averin, "Pvt- parameters of fluid inclusions and the C, O, N, and Ar isotopic composition in A garnet lherzolite xenolith from the Oasis Jetty, East Antarctica," Geochem. Int. **52** (10), 805–821 (2014).

N. V. Chalapathi Rao, R. K. Srivastava, A. K. Sinha, and V. Ravikant, "Petrogenesis of Kerguelen mantle plume-linked Early Cretaceous ultrapotassic intrusive rocks from the Gondwana sedimentary basins, Damodar Valley, Eastern India," Earth-Sci. Rev. **136**, 96–120 (2014).

M. Coffin, M. S. Pringal, R. A. Dungan, T. P. Gladczenko, M. Storey, R. D. Muller, and L. A. Gahagan, "Kerguelen hot spot magma output since 130 Ma," J. Petrol. **43** (7), 1121–1139 (2002).

P. Comin-Chiaramonti, A. Cundari, E. M. Piccirillo, C. B. Gomes, F. Castorina, P. Censi, A. Demin, A. Marzoli, S. Speziale, and V. F. Velázquez, "Potassic and sodic igneous rocks from Eastern Paraguay: their origin from the lithospheric mantle and genetic relationships with the associated Paraná flood tholeiites," J. Petrol. **38**, 495–528 (1997).

L. A. Coogan, A. D. Saunders, and R. N. Wilson, "Aluminium-in-olivine thermometry of primitive basalts: evidence of an anomalously hot mantle source for large igneous provinces," Chem. Geol. **368**, 1–10 (2014).

L. S. Egorov, "Some petrological, geochemical, and genetic features of hypabyssal alkaline-ultrabasic rocks by the example of polcenit–alkali picritic complex of the Jetty Oasis, Prince Charles Mountains, East Antarctica," Geokhimiya, No. 1, 24–39 (1994).

D. H. Elliot, T. H. Fleming, P. R. Kyle, and K. A. Foland, "Long-distance transport of magmas in the Jurassic Ferrar Large Igneous Province, Antarctica," Earth Planet. Sci. Lett. **167**, 89–104 (1999).

F. Ferraccioli, C. A. Finn, T. A. Jordan, R. E. Bell, L. M. Anderson, and D. Damaske, "East Antarctic rifting triggers uplift of the Gamburtsev Mountains," Nature **479**, 388–392 (2011).

S. F. Foley, A. V. Andronikov, and S. Melzer, "Petrology of ultramafic lamprophyres from the Beaver Lake area of Eastern Antarctica and their relation to the breakup of Gondwanaland," Mineral. Petrol. **74**, 361–384 (2002).

S. F. Foley, Dorrit E. Jacob, and Hugh St. C. O'Neill, "Trace element variations in olivine phenocrysts from Ugandan potassic rocks as clues to the chemical characteristics of parental magmas," Contrib. Mineral Petrol. **162**, 1–20 (2011). doi 10.1007/s00410-010-0579-y

S. F. Foley, D. Prelevic, T. Rehfeldt, and D. E. Jacob, "Minor and trace elements in olivines as probes into early igneous and mantle melting processes," Earth Planetary Sci. Lett. **363**, 181–191 (2013).

Geological-Geophysical Works in the Antarctic Mountainous Areas during 32 SAE: Report of NIR 61-65 (VNIIOKeanologiya, Leningrad, 1988) [in Russian].

D. A. Golynsky and A. V. Golynsky, "Rift systems of East Antarctica: a key to understanding the Gondwana break up," Regional. Geol. Metallogen. **52**, 58–72 (2012).

G. E. Grikurov, E. M. Orlenko, and L. V. Fedorov, "Alkaline-ultrabasic rocks of the Beaver Lake area, East Antarctica," Tr. *SAE* **80**, 87–99 (1980).

M. Harrowfield, G. R. Holdgate, C. J. L. Wilson, and S. McLoughlin, "Tectonic significance of the Lambert Graben, East Antarctica: reconstructing the Gondwanan Rift," Geology **33** (3), 197–200 (2005).

A. W. Hofmann, "Sampling mantle heterogeneity through oceanic basalts: isotopes and trace elements," *Treatise on Geochemistry* **2**, 61–101 (2003).

J. Hofmann, "Fault tectonics and magmatic ages in the Jetty Oasis area, Mac. Robertson Land: a contribution to the Lambert rift development," *Geological evolution of Antarctica,* Ed. by R. A. Thomson, J. A. Crame, and J. N. W. Thomson (Cambridge University Press, Cambridge, 1991), pp. 107–112.

D. A. Ionov, W. L. Griffin, and S. Y. O'Reilly, "Volatile-bearing minerals and lithophile trace elements in the upper mantle," Chem. Geol. **141**, 153–184 (1997).

R. Sh. Krymsky, D. S. Sergeev, G. E. Brügman, S. S. Shevchenko, A. V. Antonov, and S. A. Sergeev, "Experience in study of osmium isotope composition and PGE distribution in peridotites of the lithosphere mantle, East Antarctica," Regional. Geol. Metallogen. **46**, 51–60 (2011).

I. V. Kudryavtsev, A. A. Laiba, and B.V. Belyatsky, "A new dike of phlogopite alkaline picrites on the Meredith massif, Prince Charles mountains, East Antarctica," *Scientific Results of the Russian Geological–Geophysical Studies in Antarctica,* Ed. by G. L. Leitchenkov and A. A. Laiba (Politekhn, Univ., St. Petersburg, 2006), vol. 1, pp. 54–65 [in Russian].

R. G. Kurinin and G. E. Grikurov, "Structure of the rift zone of the Lambert Glacier," Tr. SAE, **80**, 76–86 (1980).

R. G. Kurinin A. S. Grinson, and Dun Tzun In, "Rift zone of the Lambert Glacier as possible alkaline-ultrabasic province in East Antarctica," Dokl. Akad. Nauk SSSR **299**, 944–947 (1988).

A. A. Laiba, A. V. Andronikov, L. S. Egorov, and L. V. Fedorov, "Stock-like and dike bodies of the alkaline-ultrabasic composition in the Jetty oasis, Prince Charles Mountains, East Antarctica," *Geological-Geophysical Studies in Antarctica* (PGO Sevmorgeologiya, Leningrad, 1987), pp. 35–46 [in Russian].

G. L. Leitchenkov, B. V. Belyatsky, A. M. Popkov, and S. V. Popov, "Geological nature of subglacial Lake Vostok in East Antarctica," *Proceedings of Glaciological Studies* **98,** 81–92 (2004).

G. L. Leitchenkov, Yu. B. Guseva V. V. Gandyukhin, S. V. Ivanov, and L. V. Safonova, "Structure of the Earth's crust and tectonic evolution history of the southern Indian Ocean (Antarctica)," Geotectonics **48** (1), 5–23 (2014).

G. L. Leitchenkov, A. V. Antonov, P. I. Lunev, and V. Y. Lipenkov, "Geology and environments of subglacial Lake Vostok," Philos. Trans. A, R. Soc. **374**, (2016) 20140302. doi 10.1098/rsta.2014.0302

G. Leitchenkov, B. Belyatsky, E. Lepekhina, A. Antonov, R. Krymsky, A. Andronikov, and S. Sergeev, "Age and isotopic marks of K-rich Manning Massif trachybasalts: an evidence for Lambert-Amery rift-system initiation (East Antarctica)," *Geophys. Research Abstracts* **19**, EGU2017-17888, EGU General Assembly 2017.

G. L. Leitchenkov, B. V. Belyatsky, and V. D. Kaminsky, "On age of the Riftogenic basaltic magmatism in East Antarctica," Dokl. Earth Sci. **478 (1)**, 11–14 (2018).

B. C. McKelvey and N. C. N. Stephenson, "A geological reconnaissance of the Radok Lake area, Amery Oasis, Prince Charles Mountains," Antarctic Sci. **2** (1), 53–66 (1990).

"Mica lamprophyre (alnoite) from Radok lake, Prince Charles Mountains, Antarctica: report: 1-6," Commonwealth of Australia. Department of National Development. Bureau of Mineral Resources, Geology and Geophysics., no. 1971/108 (1971).

N. A. Migdisova, A. V. Sobolev, N. M. Sushchevskaya, E. P. Dubinin, and D. V. Kuzmin, "Mantle heterogeneity at the Bouvet Triple Junction based on the composition of olivine phenocrysts," Russ. Geol. Geophys. **58** (11), 1289–1304 (2017).

E. V. Mikhalsky, *Proterozoic Geological Compelxes of East Antarctica: Composition and Origin,* (VNIIOkeanologiya, St. Petersburg, 2007) [in Russian].

E. V. Mikhalsky and J. W. Sheraton, "Association of dolerite and lamprophyres dykes, Jetty Peninsula (Prince Charles Mountains, East Antarctica)," Antarct. Sci. **5**, 297–307 (1993).

E. V. Mikhalsky, A. A. Laiba, and N. P. Surina, "The Lambert Province of alkaline-basic and alkaline-ultrabasic rocks in East Antarctica: geochemical and genetic characteristics of igneous complexes," Petrology **6** (5), 466–479 (1998).

E. V. Mikhalsky, J. W. Sheraton, A. A. Laiba, R. J. Tingey, D. E. Thost, E. N. Kamenev, and L. V. Fedorov, "Geology of the Prince Charles Mountains, Antarctica," Geosci. Austral. Bull. **247**, (2001).

H. Mirnejad and K. Bell, "Origin and source evolution of the Leucite Hills lamproites: evidence from Sr–Nd–Pb–O isotopic compositions," J. Petrol. **47** (12), 2460–2489 (2006).

D. A. Plavsa, S. Collins, J. F. Foden, L. Kropinski, M. Santosh, T. R. K. Chetty, and C. Clark, "Delineating crustal domains in Peninsular India: age and chemistry of orthopyroxene-bearing felsic gneisses in the Madurai Block," Precambrian Res. **198–199**, 77–93 (2012).

J. W. Sheraton, "Geochemistry of mafic igneous rocks of the northern Prince Charles Mountains, Antarctica," Aust. J. Earth Sci. **30**, 295–304 (1983).

J. W. Sheraton and R. N. England, "Highly potassic mafic dykes from Antarctica," J. Geol. Soc. Aust. **27**, 129–135 (1980).

N. W. Sheraton, W. N. Thomson, and N. D. Collerson, "Mafic dyke swarms of Antarctica," *Mafic Dyke Swarms,* Ed. by H. C. Halls and W. F. Fahrig, Geol. Ass. Canada, Sp. Pap. **34**, 419–432 (1987).

J. W. Sheraton, L. P. Black, H. M. T. McCljlin, and R. L. Oliver, "Age and origin of a compositionally varied mafic dyke swarm in the Bunger Hills, East Antarctica," Chem.Geol. **85**, 215–246 (1990).

A. V. Sobolev, A. W. Hofmann, D. V. Kuzmin, G. M. Yaxley, N. T. Arndt, S.-L. Chung, L. V. Danyushevsky, T. Elliott, F. A. Frey, M. O. Garcia, A. A. Gurenko, V. S. Kamenetsky, A. C. Kerr, N. A. Krivolutskaya, V. V. Matvienkov, I. K. Nikogosian, A. Rocholl, I. A. Sigurdsson, N. M. Sushchevskaya, and M. Teklay, "The amount of recycled crust in sources of mantle-derived melts," Science **316**, 412–417 (2007). doi 10.1126/Science.1138113

A. V. Sobolev, E. V. Asafov, A. A. Gurenko, N. T. Arndt, V. G. Batanova, M. V. Portnyagin, D. Garbe-Schönberg, and S. P. Krasheninnikov, "Komatiites reveal an Archean hydrous deep-mantle reservoir," Nature **531** (7596), 628–632 (2016). doi 10.1038/nature17152

N. C. N. Stephenson and N. D. J. Cook, "High K/Na alkaline mafic dykes near Radok Lake, northern Prince Charles Mountains, East Antarctica," Lithos **29**, 87–105 (1992).

S. -S. Sun and W. F. McDonough, "Chemical and isotopic systematics of oceanic basalts: implications for mantle composition and processes," *Magmatism in the Ocean Basins,* Ed. by A. D. Saunders and M. J. Norry, *Geol. Soc. Sp. Publ.* **42**, 313–345 (1989).

N. M. Sushchevskaya, B. V. Belyatsky, and A. A. Laiba, "Origin, distribution and evolution of plume magmatism in East Antarctica," *Volcanology,* Ed. by Fr. Stoppa (Intech Rijeka, Croatia, 2011), pp. 3–29.

N. M. Sushchevskaya, N. A. Migdisova, A. V. Antonov, R. Sh. Krymsky, B. V. Belyatsky, D. V. Kuzmin, and Ya. V. Bychkova, "Geochemical features of the Quaternary lamproitic lavas of Gaussberg Volcano, East Antarctica: result of the impact of the Kerguelen Plume," Geochem. Int. **52** (12), 1030–1048 (2014).

R. J. Tingey, "The regional geology of Archaen and Proterozoic rocks in Antarctica," *The Geology of Antarctica* (Oxford University Press, Oxford, 1991), pp. 1–73.

J. J. Veevers, "Reconstructions before rifting and drifting reveal the geological connections between Antarctica and its conjugates in Gondwanaland," Earth-Sci. Rev. **111**, 249–318 (2012).

J. J. Veevers and A. Saeed, "Permian–Jurassic Mahanadi and Pranhita–Godavari Rifts of Gondwana India: provenance from regional paleoslope and U–Pb/Hf analysis of detrital zircons," Gondwana Res. **16**, 633–654 (2009).

G. M. Yaxley, V. S. Kamenetsky, G. T. Nichols, R. Maas, E. Belousova, A. Rosenthal, and M. Norman, "The discovery of kimberlites in Antarctica extends the vast Gondwanan Cretaceous province," Nature Communications **4 (2921)**, 1–7 (2013).

Translated by M. Bogina